http://dx.doi.org/10.5012/bkcs.2012.33.10.3191

Fabrication of Amino Acid Based Silver Nanocomposite Hydrogels from PVA- Poly(Acrylamide-*co*-Acryloyl phenylalanine) and Their Antimicrobial Studies

Hyeong-Rae Cha,[†] V. Ramesh Babu,[†] K. S. V. Krishna Rao,[†,‡] Yong-Hyun Kim,[†] Surong Mei,[†,§] Woo Hong Joo,[#] and Yong-Ill Lee[†,*]

[†]*Anastro Laboratory, Department of Chemistry, Changwon National University, Changwon 641-773, Korea*
[*]*E-mail: yilee@changwon.ac.kr*
[‡]*Department of Chemistry, Yogi Vemana University, Kadapa-516003, India*
[§]*MOE Key Laboratory of Environment and Health, Institute of Environmental Medicine, School of Public Health, Tongji Medical College, Huazhong University of Science and Technology, Hubei 430030, China*
[#]*Department of Biology, Changwon National University, Changwon 641-773, Korea*
Received May 7, 2012, Accepted July 2, 2012

New silver nanoparticle (AgNP)-loaded amino acid based hydrogels were synthesized successfully from poly (vinyl alcohol) (PVA) and poly(acryl amide-*co*-acryloyl phenyl alanine) (PAA) by redox polymerization. The formation of AgNP in hydrogels was confirmed by using a UV-Vis spectrophotometer and XRD. The structure and morphology of silver nanocomposite hydrogels were studied by using a scanning electron microscopy (SEM), which demonstrated scattered nanoparticles, *ca*. 10-20 nm. Thermogravimetric analysis revealed large differences of weight loss (*i.e*., 48%) between the prestine hydrogel and silver nanocomposite. The antibacterial studies of AgNP-loaded PAA (Ag-PAA) hydrogels was evaluated against *Escherichia coli* (Gram-negative) and *Staphylococcus aureus* (Gram-positive) bacteria. These Ag-PAA hydrogels showed significant activities against all the test bacteria. Newly developed hydrogels could be used for medical applications, such as artificial burn dressings.

Key Words : Nanocomposite hydrogels, Poly(acryl amide-*co*-acryloyl phenyl alanine), Silver nanoparticles, Anti-bacterial study

Introduction

Since hydrogels possess hydrophilic character and have potential for biocompatibility, they have been of great interest to biomaterial scientists for many years.[1-4] Hydrogels have been used in numerous applications, including biosensors, bioreactors, bioseparators, tissue engineering, and drug delivery, due to their excellent biocompatibility.[5-8] Hydrophilic polymer networks are physically crosslinked or formed by crosslinking agents.[9,10] Early work in the 1980's by Yannas and coworkers[11] demonstrated the successful application of natural polymer hydrogels as artificial burn dressings. More recently, hydrogels have become attractive to tissue engineers as matrices for regenerating a wide variety of tissues and organs.[12,13] Hydrogels are hydrophilic polymer networks that may absorb water from 10-20 times (an arbitrary lower limit) up to thousands times than their dry weight.

Poly(vinyl alcohol) (PVA) is a well-known hydrophilic, biocompatible, and commercially available polymer. It has good mechanical strength, low fouling potential, and long-term temperature and pH stability. These properties of PVA lend well to its use in bioseparation, medical, and pharmaceutical applications.[14,15]

Metal nanoparticles show peculiar optical, magnetic, and electronic properties that bulk solid or isolated molecules do not usually exhibit.[16-18] Recently, there has been immense interest in the fabrication of composite materials consisting of polymer-encapsulated particles. It is now well-established that polymers are excellent host materials for nanoparticles made of metals and semiconductors.[19-21] When the nanoparticles are embedded or encapsulated in polymer, the polymer acts as a surface capping agent. The particle size is well controlled within the desired regime and make the casting of films easier.[22,23] Most popular methods employed for encapsulation include emulsion polymerization, surfactant-free emulsion polymerization, emulsion-like polymerization, suspension polymerization, and dispersion polymerization. Among metal/polymer composites, silver composites have found important applications in material technologies like optical materials,[24] catalytic systems, antibacterial materials,[25,26] chemical nanosensors, and surface-enhanced Raman scattering (SERS).[27] However, the most significant challenge encountered in preparing silver/polymer nanoparticle encapsulation is that the nanoparticles cannot be dispersed in polymer matrix at the nano level by conventional techniques because the surface energies of tiny silver particles are very high, and these particles tend to agglomerate during mixing. For application in optoelectronics and electronics, the precise control of particle size and their uniform distribution within the polymer are key technologies based on nanoparticles in polymers. Improved stability of silver nanoparticles (AgNPs) has been understood in polystyrene (PS),[28,29] possibly because of the presence of

free electrons in the functional groups of the polymer chains, which allow the particles to be held more firmly by the functional groups. Selection of antibacterial material is important for medical materials or hygienic appliances. AgNPs are excellent antibacterial materials. However, the preparation of AgNP is difficult because they agglomerate easily.

L-Phenylalanine is an essential amino acid and a tyrosine precursor that acts in the central nervous system as an antidepressant and mood elevator.[30] The phenyl group of the phenylalanine residue should provide a rather large hydrophobic domain in which cohesive forces play major roles during the conformational transitions of macromolecules. The magnitude of the hydrophobic character may also be revealed by calorimetric data. Thus, a thermodynamic study is of special interest, because it enables correlations to be established between increasing hydrophobicity and the appearance of a compact structure.[31,32] In the present study, we developed AgNPs in semi-IPN hydrogels composed of acrylamide and acryloyl phenylalanine in the presence of polyvinyl alcohol. The encased silver particles demonstrated very good antibacterial properties.

Experimental

Materials. Poly (vinyl alcohol) (MW=125,000), acrylamide (AAm), *N,N'*-methylenebisacrylamide (MBA), ammonium persulfate (APS), silver nitrate ($AgNO_3$), L-phenyl alanine, and 2,6-di-*tert*-butyl-*p*-cresol were purchased from Aldrich, USA. Sodium borohydride ($NaBH_4$) was purchased from Acros Organics, Japan.

Synthesis of PVA-P(AAm-*co*-APA) Hydrogels. PVA/AAm-*co*-APA (PAA) hydrogels with different compositions and crosslinking agent concentrations (Figure 1) were prepared by radical polymerization. *N*-Acryloloyl-L-phenylalanine (APA) was prepared according to published procedures.[33] A 6 wt % PVA aqueous solution was prepared in double distilled water at 80 °C. After dissolution, the solution was cooled to room temperature and different amounts of APA and AAm were added. Cross linking agent (MBA, 0.12 mmol) and initiator (KPS, 0.36 mmol) were added to this reaction mixture, followed by stirring. The resulting solution was stirred for 2 h, and then allowed to polymerize at 35 °C for three days. After completion of polymerization, 3 mm cylinder-shaped hydrogels were immersed in distilled water for four days. The water was changed every 12 h in order to remove residual monomers. The swollen gels were dried under vacuum oven at 40 °C to attain a constant weight.

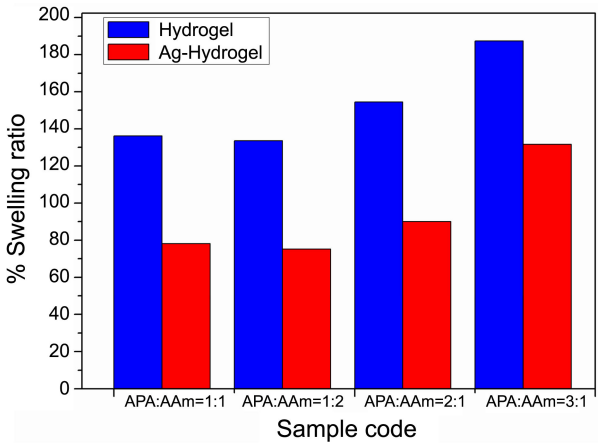

Figure 1. The influences of acrylamide and *N*-Acryloloyl-L-phenylalanine (APA) ratios on the swelling characteristics of PAA hydrogels and Ag-PAA hydrogels.

Fabrication of Ag Nanoparticles in PAA Hydrogels. Dried PAA hydrogels were immersed in distilled water for three days at room temperature. Freshly swollen gel discs were equilibrated in 50 mL of $AgNO_3$ aqueous solution (0.005 M) for 24 h. The gel discs were transferred into 50 mL of 0.05 M $NaBH_4$ aqueous solution for 2-3 h to reduce the $AgNO_3$ into Ag colloidal particles. The developed Ag nanoparticle loaded PAA hydrogels designated as Ag-PAA.

Swelling Studies. Fully dried pristine PAA hydrogels and Ag-PAA hydrogels were weighed and equilibrated in distilled water at 37 °C for three days. The equilibrium swelling capacity or swelling ratio (Q) of the hydrogel was calculated employing the following Eq. (1);[34]

$$Q = W_e/W_d \quad (1)$$

where, W_e is the swollen PAA hydrogels weight and W_d is the dry PAA hydrogels.

Characterization. UV-visible spectra of PAA hydrogel and Ag-PAA hydrogels (4 mg in 1 mL of distilled water) were accomplished using an Agilent 8453 UV spectrophotometer. X-ray diffraction measurements of samples were carried out using a X'pert MPD 3040. The thermal properties of Ag-PAA hydrogels were evaluated using a TA 5000/SDT 2960 thermal analyzer (Zurich, Switzerland) at a heating rate of 10 °C/min under nitrogen atmosphere (flow rate 10 mL/min). Morphological studies of dry hydrogel and Ag-PAA hydrogels were performed with a MIRA LMH, H.S scanning electron microscope (SEM) and a JEM 2100F transmission electron microscope (TEM).

Antibacterial Studies. Antibacterial activity screen studies of placebo Ag-PAA hydrogel and its Ag nanoparticle (AgNP)-hydrogels were conducted by the paper disc method. A quantity of 5 mL of nutrient agar (NA) medium (pH = 6.8) was poured into sterilized plates and allowed to solidify. The plates were inoculated with spore suspensions of *Escherichia coli* (*E. coli*) and *Staphylococcus aureus* (*S. aureus*) paper discs (8 mm diameter) were placed inside the culture plates by a sterilized cork borer. The Ag nanoparticle (AgNP)-hydrogel solutions (10 mg/10 mL and 20 mg/20 mL distilled water) absorbed discs were placed on cultured agar plates. The plates were examined for possible clear zone formation after incubation at 37 °C for one day. At the end of the incubation period, the diameters of inhibition zones occurred on the medium were evaluated in millimeters. The measuring process was repeated five times and results were averaged. To calculate the antibacterial activity of these newly prepared Ag nanoparticle (AgNP)-hydrogels statistically, we

used the following standard Eq. (1) to measure the inhibition zone.

$$\bar{x} \pm \frac{ts}{\sqrt{n}} \quad (1)$$

Where, n is the number of observations, s is the measured standard deviation, $\bar{x}$ is the measured mean value of the inhibition zone, and t is Student's t (t = 2.776 at 95% confidence level).

Results and Discussion

The present approach involves the incorporation of amino acid moiety as in the form of monomer, such as APA, which is having acidic in nature. The silver nanocomposite hydrogels composed from PVA-P(Am-*co*-APA) (Ag-PAA) and it is schematically represented in Scheme 1. PVA is a charge stabilizer for hydrogel formation. The functional groups presented in APA and AAm molecules were responsible for the reduction of silver salts into AgNPs, and were also capable of providing additional stabilization through high molecular chains. The strong interaction with silver likely involve with oxygen and nitrogen. By using sodium borohydride, a strong reducing agent, PAA hydrogel matrix provides steric protection due to the network and bulkiness of the matrix *via* direct bonding with these electron donor sites. Various natural and synthetic hydrophilic polymers containing hydroxyl (-OH), carboxylic (-COOH), amino (-NH_2), or thiol (-SH) groups could offer reduction capacities in addition to stabilizing the formed nanoparticles.

Figure 1 shows the influence of acrylamide and APA ratios on the swelling characteristics of pristine PAA hydrogels and Ag-PAA hydrogels. Reasonable variation was observed in the swelling ratios of hydrogels. The swelling ratios were observed in the following order of pristine PAA hydrogels (137-187%) > Ag-PAA hydrogels (75-130%). The swelling behaviors of hydrogels varied with differing monomer ratios. The swelling ratio increases with increasing APA concentration due to increases in the hydrophilicity of the hydrogel network.

When reducing silver ions into AgNPs in the PAA hydrogel networks using $NaBH_4$, the hydrogel networks solution color immediately turned brown. The UV-visible absorption studies confirmed the formation of Ag-PAA hydrogels as

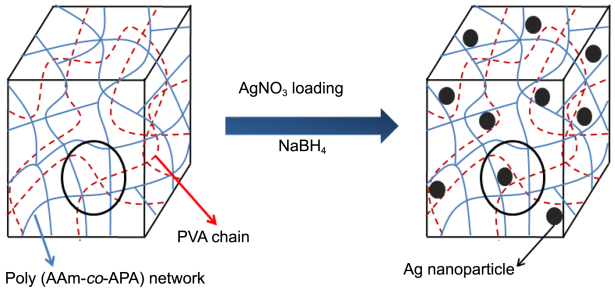

Scheme 1. Schematic representation of the synthesized Ag-poly(acryl amide-*co*-acryloyl phenyl alanine) (PAA) hydrogel network.

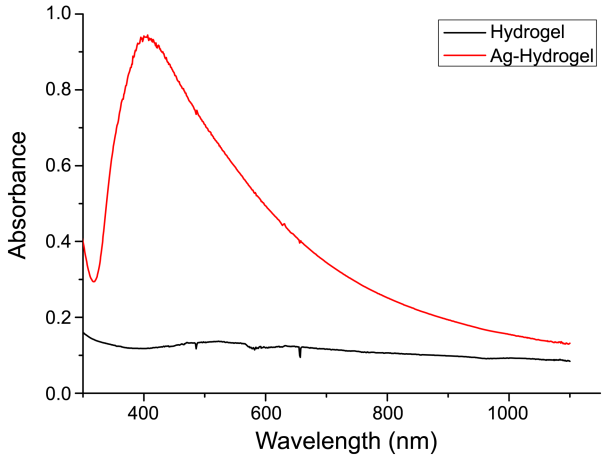

Figure 2. UV-visible spectra for PAA hydrogel and Ag-PAA hydrogels.

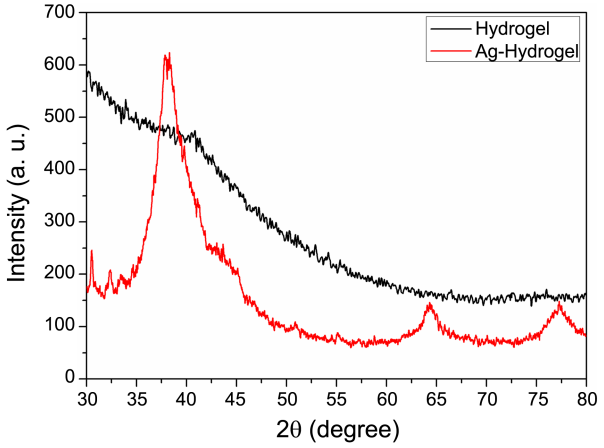

Figure 3. XRD patterns of PAA hydrogel and Ag-PAA hydrogels.

shown in Figure 2. An absorption peak at around 400 nm confirmed AgNPs due to the surface plasmon resonance (SPR) effect, whereas pure hydrogel did not show any significant absorption in the UV-visible spectrum.[35,36] X-ray diffraction patterns of PAA hydrogels and Ag-PAA nanocomposite hydrogels are given in Figure 3. The XRD diffractogram of Ag-PAA hydrogels are assigned to diffractions at 2θ values at 39.87°, 64.47°, and 77.33° are due to (111), (220), and (311) planes of the face-centered cubic (fcc) silver, respectively, whereas absence of peaks in pristine PAA hydrogels confirmed the non-crystalline nature.[34,37] Another peak around 44.23° also appoints (200) plane of Ag fcc even though it is very weak in this region. The TGA curves of pure PAA hydrogel and Ag-PAA hydrogels are presented in Figure 4. Ag-PAA hydrogel showed an enhanced thermal stability, resulting in only a 45% weight loss below 400 °C in three degradation steps. The pristine PAA hydrogel followed three decomposition steps, and 80% degradation of the hydrogel chains occurred below 500 °C. The weight loss or difference in decomposition between the hydrogel and Ag-PAAhydrogel was found to be 48%, and illustrates the presence of AgNPs (weight loss) in the hydrogel. This difference is significant and has not been previously observed.[38]

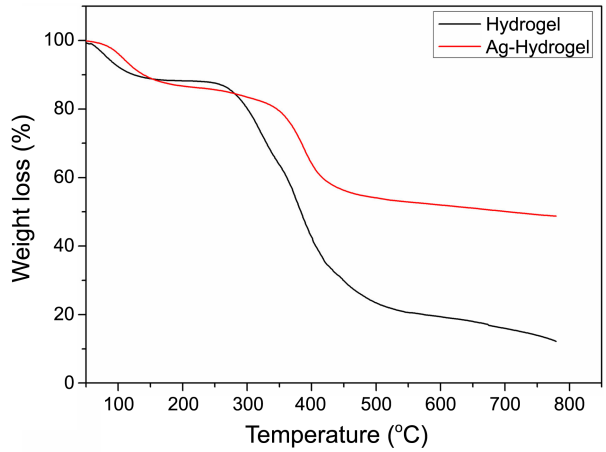

Figure 4. TGA curves of PAA hydrogel and Ag-PAA hydrogels.

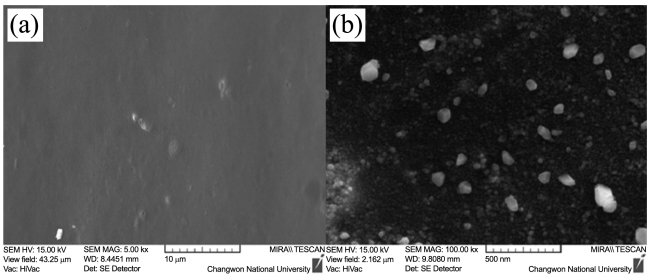

Figure 5. The SEM images of (a) pristine PAA hydrogel and (b) Ag-PAA hydrogel nanocomposites.

To confirm visually that AgNPs were formed in the hydrogel matrix, hydrogels impregnated with AgNPs were scanned *via* SEM. Figure 5 demonstrates SEM images of PAA hydrogels and Ag-PAA hydrogel nanocomposites. A clear surface of the pure hydrogel can be observed in Figure 5(a). On the other hand, Figure 5(b) demonstrates the rocky surface of the Ag-PAA hydrogel due to the presence of AgNPs inside the gel networks. However, there is little variation in the case of AgNPs formed in the gel networks, which illustrates the formation of defined nanostructures in the hydrogel networks. The formation of AgNPs clearly indicates the polymer matrix rather than simply nanoparticles entrapped in the hydrogel networks. The size of AgNPs are commonly controlled by varying the monomer ratio and hydrophilicity of hydrogel.

A TEM graph illustrates the distribution of AgNPs (Figure 6(a)). It is possible that the AgNPs formed in the cross-linked networks are spherical, highly dispersed, and few nanometers in size. Moreover, the selected area electron diffraction (SAED) pattern of AgNPs in Figure 6(b) is clearly visible as three diffraction rings from the selected area of the TEM image, and they are definitely attributed to the face-centered cubic structures of AgNPs. The brightest ring and the one closest to the center is a combination of the (111) and (200) reflections. The second ring belongs to the (222) reflection and the weakest third ring is due to either (420) and/or (422) reflections. This ultimately helps not only in controlling the size of the nanoparticles, but also provides

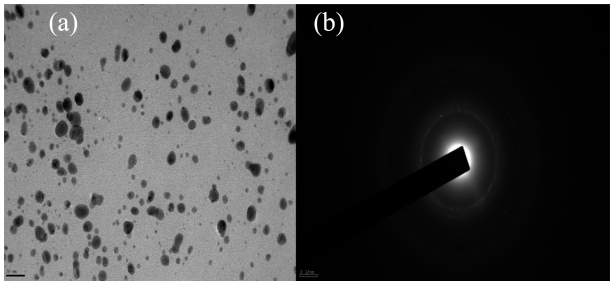

Figure 6. (a) TEM image of silver nanoparticles obtained from Ag-PAA hydrogel nanocomposites. (b) The selected area electron diffraction (SAED) pattern of Ag-PAA hydrogel nanocomposites.

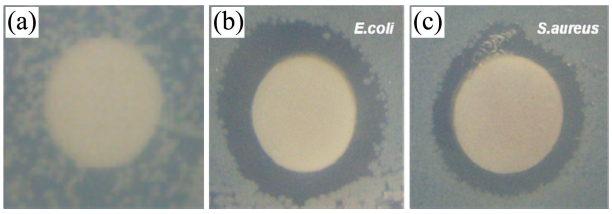

Figure 7. Photographs of (a) cultured *Escherichia coli* in nutrient agar medium and anti-bacterial screeing of the Ag-PAA hydrogels against (b) *E. coli* and (c) *S. aureus*.

better stabilization of nanoparticles for longer periods. In this environment, the PVP chains in the networks are highly compact in nature and provide enough stability to the AgNPs. The sizes of most Ag nanoparticles are found between 10 and 20 nm.

The antibacterial effect of the placebo PAA hydrogel and Ag-PAA hydrogels was investigated by comparing the diameter of growth inhibition zone with cultured *Escherichia coli* and *Staphylococcus aureus* in nutrient agar medium before and after adding Ag-PAA hydrogels at concentrations of 1.0 mg/mL and 2.0 mg/mL. Figure 7 illustrates the photographs of *in-vitro* antibacterial screening for the Ag-PAA hydrogel nanocomposite, which were carried out against *E. coli and S. aureus.* No obvious antibacterical effect of the placebo Ag-PAA hydrogel was observed. However, apparent antibacterial activity of silver-hydrogel nanocomposite was noted against *E. coli* and *S. aureus*. The diameter of growth inhibition zone were 12.8 ± 0.3 mm against *E. coli* and 11.6 ± 0.3 mm against *S. aureus* with 1.0 mg/mL of Ag-PAA hydrogel nanocomposite. The antibacterical ability was enhanced with increasing the concentration of the silver-hydrogel nanocomposite (13.6 ± 0.2 mm against *E. coli* and 12.4 ± 0.2 mm against *S. aureus* with 2.0 mg/mL of Ag-PAA hydrogel nanocomposite). These results suggest that the silver nanocomposite hydrogel showed a more toxic effect than placebo hydrogel under similar conditions. The possible mode of increased toxicity of the silver-hydrogel may be due to interactions of the AgNPs with the lipid layer of cell membranes.

Conclusions

In the present study, we fabricated well-dispersed and

stable AgNPs using PVA-poly(acrylamide-*co*-acryloyl phenylalanine) networks. XRD studies, thermal analysis, and UV-visible spectra revealed the formation of AgNPs in the hydrogel matrixes. SEM and TEM images showed the narrow distributions and spherical shapes of AgNP. The developed nanoparticles showed good antibacterial activity. Hence we conclude that the prepared hydrogel nanocomposites are excellent potential candidates for medical applications, such as artificial burn dressings.

Acknowledgments. This work was supported by the Priority Research Centers Program through the National Research Foundation of Korea (NRF) funded by the Ministry of Education, Science and Technology (NRF 2010-0029634) and Changwon National University (2011).

References

1. Deligkaris, K.; Tadele, T. S.; Olthuis, W. *J. Sensor. Actuat. B* **2010**, *147*, 765.
2. Song, F. L.; Zhang, M.; Shi, J. F.; Li, N. N.; Yang, C.; Li, Y. *Mater. Sci. Eng. C* **2010**, *30*, 804.
3. Pourjavadi, A.; Hosseinzadeh, H. *Bull. Korean Chem. Soc.* **2010**, *31*, 3163.
4. Krebs, M. D.; Jeon, O.; Alsberg, E. *J. Am. Chem. Soc*. **2009**, *131*, 9204.
5. Jo, S. Y.; Lim, Y. M.; Youn, M. H.; Gwon, H. J.; Park, J. S.; Nho, Y. C.; Shin, H. *Polym.-Korea* **2011**, *33*, 551.
6. Skardal, A.; Sarker, S. F.; Crabbé, A.; Nickerson, C. A.; Prestwich, G. D. *Biomaterials* **2010**, *31*, 8426.
7. Huang, R.; Kostanski, L. K.; Filipe, C. D. M.; Ghosh, R. *J. Membrane Sci.* **2009**, *336*, 42.
8. Hirose, M.; Tachibana, A.; Tanabe, T. *Mater. Sci. Eng. C* **2010**, *30*, 664.
9. Rossi, F.; Perale, G.; Storti, G.; Masi, M. *J. Appl. Polym. Sci*. **2012**, *123*, 2211.
10. Moon, J. R.; Kim, B. S.; Kim, J. H. *Bull. Korean Chem. Soc.* **2006**, *27*, 981.
11. Yannas, I. V.; Lee, E.; Orgill, D. P. *Proc. Natl. Acad. Sci. USA* **1989**, *86*, 933.
12. Hubbell, J. A. *Curr. Opin. Sol. State Mater. Sci* **1998**, *3*, 246.
13. Kim, B. S.; Nikolovski, J.; Bonadio, J.; Mooney, D. J. *Nature Biotech*. **1999**, *17*, 979.
14. Xia, C.; Xiao, C. *J. Appl. Polym. Sci*. **2012**, *123*, 2244.
15. Liu, Z.; Liu, J.; Chen, T. *Sensor. Actuat. B* **2005**, *107*, 311.
16. Temgire, M. K.; Joshi, S. S. *Radiat. Phys. Chem*. **2004**, *71*, 1039.
17. Zhan, W. Z.; Qiao, X. L.; Chen, J. G. *J. Colloid Interface Sci.* **2006**, *302*, 370.
18. Ledo, A.; Martinez, F.; Quintela, M. A. L. *J. Phys. B* **2007**, *398*, 273.
19. Brandt, K.; Salikov, V.; Ozcoban, H.; Staron, P.; Schreyer, A.; Prado, L. A. S. A.; Schulte, K.; Heinrich, S.; Schneider, G. A. *Composite Sci. Tech*. **2011**, *72*, 65.
20. Liang, G. D.; Bao, S. P.; Tjong, S. C. *Mater. Sci. Eng. B* **2007**, *142*, 55.
21. Hong, Y.; Ding, S. J.; Wu, W.; Hu, J. J.; Voevodin, A. A.; Gschwender, L.; Snyder, E.; Chow, L.; Su, M. *ACS Appl. Mat. Inter*. **2010**, *2*, 1685.
22. Paik, Y.; Poliks, B.; Rusa, C. C.; Tonelli, A. E.; Schaefer, J. *J. Polym. Sci. Part B: Polym. Phys*. **2007**, *45*, 1271.
23. Zhao, C. J.; Zhao, Q. T.; Zhao, Q. Z. *J. Photochem. Photobiol. A* **2007**, *187*, 146.
24. Endo, T.; Ikeda, R.; Yanagida, Y.; Hatsuzawa, T. *Anal. Chim. Acta* **2008**, *611*, 205.
25. Zhang, C.; Yang, Q.; Zhan, N.; Sun, L.; Wang, H.; Song, Y.; Li, Y. *Colloids and Surfaces A: Physicochem. Eng. Aspects* **2010**, *362*, 58.
26. Basri, H.; Ismail, A. F.; Aziz, M.; Nagai, K.; Matsuura, T.; Abdullah, M. S.; Ng, B. C. *Desalination* **2010**, *261*, 264.
27. Setua, P.; Chakraborty, A.; Seth, D. *Phys. Chem. C* **2007**, *111*, 3901.
28. Khanna, P. K.; Singh, N.; Charan, S.; Viswanath, A. K. *Mater. Chem. Phys*. **2005**, *92*, 214.
29. Yilmazer, U.; Ozden, G. *Polym. Compos.* **2006**, *27*, 249.
30. Sabelli, H. C. *J. Clin. Psychiatry* **1991**, *52*, 137.
31. Methenitis, C.; Morcellet, J.; Pneumatikakis, G.; Morcellet, M. *Macromolecules* **1994**, *27*, 1455.
32. Barbucci, R.; Casolaro, M.; Magnani, A. *Chem. Rev.* **1992**, *120*, 29.
33. Casolaro, M.; Paccagnini, E.; Mendichi, R.; Ito, Y. *Macromolecules* **2005**, *38*, 2460.
34. Murali, M. Y.; Premkumar, T.; Lee, K. J.; Geckeler, K. E. *Macromol. Rapid Commun.* **2006**, *27*, 1346.
35. Mostafavi, M.; Keghouche, N.; Delcourt, M. O.; Belloni, J. *Chem. Phys. Lett.* **1990**, *167*, 193.
36. Gutierrez, M.; Henglein, A. *J. Phys. Chem. B* **1993**, *97*, 11368.
37. Leff, D. V.; Brandt, L.; Heath, J. R. *Langmuir* **1996**, *12*, 4723.
38. Yin, W.; Yanga, H.; Cheng, R. *Eur. Phys. J*. **2005**, *E17*, 1.